Microlensing of Gamma Ray Bursts by Stars and MACHOs

Edward A. Baltz[1] and Lam Hui[2]

ABSTRACT

The microlensing interpretation of the optical afterglow of GRB 000301C seems naively surprising, since a simple estimate of the stellar microlensing rate gives less than one in four hundred for a flat $\Omega_\Lambda = 0.7$ cosmology, whereas one event was seen in about thirty afterglows. Considering baryonic MACHOs making up half of the baryons in the universe, the microlensing probability per burst can be roughly 5% for a GRB at redshift $z = 2$. We explore two effects that may enhance the probability of observing microlensed gamma-ray burst afterglows: binary lenses and *double* magnification bias. We find that the consideration of binary lenses can increase the rate only at the $\sim 15\%$ level. On the other hand, because gamma-ray bursts for which afterglow observations exist are typically selected based on fluxes at widely separated wavebands which are not necessarily well correlated (e.g. localization in X-ray, afterglow in optical/infrared), magnification bias can operate at an enhanced level compared to the usual single–bias case. Using a simple model for the selection process in two bands, we compute the enhancement to microlensing rate due to magnification bias in two cases: perfect correlation and complete independence of the flux in the two bands. We find that existing estimates of the slope of the luminosity function of gamma-ray bursts, while as yet quite uncertain, point to enhancement factors of more than three above the simple estimates of the microlensing rate. We find that the probability to observe at least one microlensing event in the sample of 27 measured afterglows can be $3 - 4\%$ for stellar lenses, or as much as $25\,\Omega_{\rm lens}$ for baryonic MACHOs. We note that the probability to observe at least one event over the available sample of afterglows is significant only if a large fraction of the baryons in the universe are condensed in stellar–mass objects.

Subject headings: gamma rays:bursts — gravitational lensing – binaries: general

1. Introduction

The optical afterglow of GRB 000301C, at a redshift of $z = 2.034$, exhibited variability prior to the break in the power law decline in its lightcurve. This variability has been interpreted as

[1]KIPAC, Stanford University, P.O. Box 90450, MS 29, Stanford, CA 94309, eabaltz@slac.stanford.edu

[2]NASA/Fermilab Astrophysics Center, Fermi National Accelerator Laboratory, PO Box 500, Batavia, IL 60510 lhui@fnal.gov

gravitational microlensing (Garnavich, Loeb & Stanek 2000), as first proposed by Loeb & Perna (1998). While there is no obvious intervening galaxy which might provide lenses in the form of stars or MACHOs, we will take this possibility seriously. Koopmans and Wambsganss (2001) considered lensing by MACHOs (see also Wyithe & Turner (2002b)), but as we will explain in §7 we find a rate of MACHO lensing five times larger than theirs. The rate of microlensing by stars is much lower, and is naively of order one in three hundred GRBs at redshift two. We note that microlensing is not the only possible explanation of this lightcurve (Panaitescu 2001). Several authors have considered using microlensing to study the properties of the underlying afterglow (Granot & Loeb 2001; Gaudi & Loeb 2001; Gaudi, Granot & Loeb 2001; Ioka & Nakamura 2001). In this work we will only make statements about afterglows in the aggregate.

Assuming that there is a fraction $f \sim 0.1 - 0.2$ of dark matter in MACHOs, it is not surprising that a lensing event was seen. However, if the only cosmological microlenses are stars, the observation of an event is somewhat problematic. Roughly thirty afterglows have been well–characterized (starting with Metzger et al. (1997) and Kulkarni et al. (1998) and summarized in Frail et al. (2001) and Bloom, Frail & Kulkarni (2003)). We investigate whether magnification bias can make a significant difference, considering the two extreme possibilities that the optical and gamma ray fluxes are perfectly correlated or perfectly uncorrelated. In Appendix A we consider binary lenses, as discussed by Mao & Loeb (2001). Neither of these two effects seems to be able to increase the probability by a factor of ten. We thus conclude that the observation of a second microlensing event by a star in a sample twice as large is quite unlikely, though with a large MACHO fraction the probability can be significant.

In §2 we summarize the basic physics involved in gamma ray burst fireballs, and give an overview of the multiwavelength observations. In §3 we derive the cosmological microlensing rate (relegating the details for binary lenses to Appendix A). In the remaining sections (§4 – §6) we discuss the enhancement of the lensing probability due to magnification bias (Turner, Gott & Ostriker 1984). Magnification bias is the effect that a given *detected* source is more likely to be lensed than a source chosen randomly, simply because magnified sources are easier to detect. We will consider both the usual single magnification bias, as well as double magnification bias which might be relevant here because of the way gamma-ray burst afterglows are selected. The selection is complicated, involving gamma ray, X-ray and optical wavelengths. We can only hope to capture the basic features. In §4 & §5 we consider how the magnification bias affects bursts at a single redshift, while in §6 we consider the magnification bias on the sample of well–measured afterglows in Bloom et al. (2003).

We primarily consider the gravitational lensing caused by point mass lenses. We define the distance to the source D_s, lens D_ℓ, and deflector–source distance $D_{\ell s}$. These distances are all angular diameter distances in physical units, and we take a flat cosmology where $\Omega_m + \Omega_\Lambda = 1$. We define the Einstein radius and the Einstein angle for the system as

$$R_E = \sqrt{\frac{4GM}{c^2}\frac{D_\ell D_{\ell s}}{D_s}}, \qquad \theta_E = \frac{R_E}{D_\ell}, \tag{1}$$

where M is the mass of the point lens.

2. Physics and Observations of GRB Afterglows

The basic picture of a gamma-ray burst (GRB) afterglow is a fireball with a relativistic jet with some small opening angle (e.g. Waxman 1997a). The observed afterglow light is emitted in a ring of opening angle $1/\gamma$, where γ is the Lorentz factor of the ejecta moving at velocity v. This ring expands at an apparent rate $v_{\rm app} = \gamma v$, the so–called superluminal expansion. This superluminal expansion is what allows for rapid microlens variability, even at cosmological distances (Loeb & Perna 1998).

We take the radius of the afterglow ring in units of the Einstein radius from Waxman (1997b) and Garnavich et al. (2000),

$$R(t) = 0.50 \left(\frac{E_{53}}{n_1}\right)^{1/8} (1+z_s)^{-5/8} \left(\frac{M_{\rm lens}}{M_\odot}\right)^{-1/2} \left(\frac{D_\ell D_{\ell s}/D_s}{c/H_0}\right)^{-1/2} t_{\rm day}^{5/8}, \qquad (2)$$

where E_{53} is the isotropic burst energy in units of 10^{53} ergs, and n_1 is the ambient gas density in units of 1 cm^{-3}. We will assume for this work that we want a microlensing event to occur at some minimum time after the GRB, to allow for optical observations. To enforce this assumption we take $R > 0.2$, typically achieved roughly one tenth day after the burst at a redshift of $z = 2$. We define the fractional apparent width of the emitting region w, where the emission comes in the annulus between $R(1-w)$ and R. In fact, there is some emission throughout the interior of the ring, but the inner part is less bright (Granot, Piran & Sari 1999).

For our later calculation, we need to know the intrinsic (not apparent) luminosity function of GRBs, at different wavebands. This is a subject of much uncertainty at the moment. Schaefer, Deng & Band (2001) found that the luminosity function $N(L) \equiv dn/dL$ at gamma-ray energies is a power law of slope -1.7 at the faint end. This result is obtained by assuming a lag–variability relation. Note that bursts of all durations are included in their analysis, whereas bursts for which afterglows have been observed fall into the long duration category (as localization of the bursts is typically done with BeppoSAX observations which are insensitive to bursts with durations less than about a second). Frail et al. (2001) demonstrated using about 20 afterglows that the total energy output is remarkably constant from burst to burst, about 5×10^{50} ergs, most of which comes out in gamma-ray. Bloom et al. (2003) confirmed this result with a larger sample of about 30 afterglows. However, what is important to us is not the true total energy, but rather the isotropic equivalent energy. It is the latter that determines the effective luminosity of the burst (i.e. the observed fluence is proportional to the isotropic equivalent energy divided by the luminosity distance squared). The two are related via a geometrical factor determined by the opening angle of the burst. The luminosity function is therefore determined by the distribution of opening angles. Frail et al. (2001) derived this distribution using the observed jet break times. However, it is important to

keep in mind that the distribution of opening angles is obtained from a flux-limited sample.[3] To relate that to the intrinsic distribution of opening angles, and therefore luminosities, would require detailed modeling of the selection, which is beyond the scope of this paper.[4] Krumholz, Thorsett & Harrison (1998) derived constraints on the GRB luminosity function by matching the number-peak-flux relation in the BATSE catalog (see also Rutledge, Hui & Lewin 1995), as well as making use of three bursts with known redshifts at the time. Assuming that the redshift distribution follows the global star formation history (see Madau et al. 1996; Madau, Pozzetti & Dickinson 1998; Wijers et al. 1998), they find that a power-law slope of -1.6 to -2.05 is consistent with observations (see Fig. 1 in Krumholz et al. 1998).

The luminosity function at optical wavebands is even more uncertain, because of the limited number of afterglows. On theoretical grounds, one expects the gamma-ray emission to be well correlated with X-ray, but not with the optical. This is because the X-ray frequencies are generally above the various characteristic frequencies of the relativistic fireball, such as e.g. the synchrotron self–absorption frequency, whereas the (unknown) relative ordering of the characteristic frequencies affects the optical flux significantly. Some observational evidence of this can be found in Freedman & Waxman (2001) (see also useful discussions in Kumar (2000) and Sari, Piran & Narayan (1998)). For our later investigation, we will examine both the case where the gamma-ray / X-ray and optical emission are well-correlated, and the case where they are not. As far as the slope of the optical luminosity function is concerned, we will assume, for simplicity and the lack of evidence to the contrary, it is the same as that for the gamma-ray emission.

Observation of an optical afterglow has a complicated selection process, which we will outline here. First, the burst is detected in gamma-rays (> 20 keV or so) by BATSE, but it is at lower X-ray energies that the bursts are localized by e.g. BeppoSAX. After a localization, an attempt to measure the optical afterglow can be made. Thus, to detect an optical afterglow, there are effectively three thresholds that must be exceeded. The gamma-ray and X-ray fluxes are believed to be well–correlated, but the correlation with the optical flux is uncertain (Granot & Sari 2002).

3. Microlensing Rate

The microlensing optical depth is defined as the number of lenses within some minimum impact parameter of the line of sight to an object. The basic optical depth, where the impact parameter is

[3]The sample is heterogeneous in nature, assembled from observations by a variety of groups under different conditions. To the extent that faint GRBs are less likely to be observed, one can regard the sample as crudely flux-limited.

[4]It is worth noting that the luminosity function obtained directly from a flux limited sample with no corrections is always biased against faint sources (even if the source redshifts are known), typically driving the inferred function flatter than the true one.

taken to be an Einstein radius, is given by the following for a flat cosmology (Press & Gunn 1973):

$$\tau_0 = \frac{3}{2}\Omega_{\rm lens}\int_0^{z_s}\frac{dz_\ell\,(1+z_\ell)}{\sqrt{\Omega_m(1+z_\ell)^3+\Omega_\Lambda}}\frac{\chi_\ell(\chi_s-\chi_\ell)}{\chi_s}, \tag{3}$$

where χ is the dimensionless coordinate distance, i.e. the luminosity distance is $D_L = c\chi(1+z)/H_0$. In Fig. 1 we plot the optical depth as a function of redshift for several values of Ω_m in a flat cosmology, dividing out the $\Omega_{\rm lens}$ dependence. The quantity $\Omega_{\rm lens}$ is the fraction of critical density today that is in objects capable of causing microlensing. We have assumed that the comoving number density of such objects is constant – if it decreases towards higher redshifts, the optical depth will be lower. For $\Omega_m = 0.3$ and $z = 2$, the optical depth is $\tau_0 = 0.65\,\Omega_{\rm lens}$. Fukugita, Hogan & Peebles (1998) estimated $\Omega_{\rm lens}$ in stars to be $\Omega_{\rm lens} \approx 0.0035$. With this value, constant out to redshift $z = 2$, the optical depth is 1/440 for $\Omega_m = 0.3$, and is as large as 1/260 for $\Omega_m = 0.1$, though the latter value for the matter density is strongly disfavored. For MACHOs, we will simply assume that $\Omega_{\rm lens} = f\Omega_m$, namely that the halo MACHO fraction is universal. According to Fukugita et al. (1998), roughly half of the baryons are accounted for at redshift zero, so the density of baryonic MACHOs should not exceed $\Omega_b/2 \approx 0.01h^{-2}$, and thus $f \leq 1/15$ for $\Omega_m = 0.3$ and $h = 0.7$. Of course non-baryonic MACHOs could have $f = 1$. We will thus take $\Omega_{\rm lens} = 0.02$ as the largest plausible value, though even this value has problems (Graff et al. 1999; Fields, Freese & Graff 2000). There are limits on the cosmological abundance of MACHOs of any kind (Dalcanton et al. 1994), but $\Omega_{\rm lens} < 0.1$ is allowed for stellar–mass lenses. In the baryonic case, the optical depth to redshift $z = 2$ is as large as 1/75, which is not excessively smaller than the observed rate.

Though we discussed excising the central region $R < 0.2$ of the Einstein ring in the previous section, to account for afterglow lensing events that happen too quickly to be detected, doing so has only a small effect on the rate, in fact this region is only 4% of the Einstein ring. This cut will have a larger effect in the next section, where we will be discussing magnification bias.

The actual optical depth of relevance depends on the magnification one is interested in. Assuming A_0 is the magnification threshold of interest, the optical depth is:

$$\tau = \tau_0\int_0^\infty du\,\Theta\left[A_{\rm max}\left(\sqrt{u}\right) - A_0\right] = \tau_0\beta^2. \tag{4}$$

where $A_{\rm max}$ is the peak magnification for the given lens system at a distance $r = \sqrt{u}$ in Einstein units from the burst. Here, β is the distance from the lens in Einstein units where the peak magnification is A_0. The symbol $\Theta(x)$ denotes a step function (= 1 if $x \geq 0$, and zero otherwise). Ignoring magnification bias, the optical depth τ is equal to the rate of microlensed GRBs. For GRB 000301C, the peak magnification was approximately $A_0 = 2$.

In Table 1 we give the optical depth to lensing for several different magnification thresholds and we also consider three cases for the fractional width of the emitting ring in the gamma ray burst afterglow. We find that the consideration of binary lenses typically increases the optical depth, but not by a large amount (see Appendix A). The two main effects that we see are that binaries give a

larger increase for narrower source rings, and a larger increase for larger thresholds. Note that for this calculation, we only require that the peak magnification exceed the threshold, and we do not consider the detailed structure of the lightcurve.

In the remainder of this paper, we will assume that $\Omega_m = 0.3$, $A_0 = 2$ and $w = 0.1$, which gives $\tau = 1.4\tau_0$. We will consider both stellar lenses with $\Omega_{\rm lens} = 0.0035$ and MACHOs with $\Omega_{\rm lens} = f\Omega_m$.

For microlensing of point sources, the probability of an impact parameter less than β in Einstein units, and thus a magnification greater than $A = (2+\beta^2)/\sqrt{\beta^2(4+\beta^2)}$ is simply given by

$$P = 1 - e^{-\tau_0\beta^2} \approx \tau_0\beta^2. \tag{5}$$

We will use the approximate expression, and thus we need to truncate to ensure that $P \leq 1$,

$$P = 2\tau_0 \left(\frac{A}{\sqrt{A^2-1}} - 1 \right) \Theta \left(A - \frac{1+2\tau_0}{\sqrt{1+4\tau_0}} \right). \tag{6}$$

The probability density corresponding to this expression is now

$$\frac{dP}{dA} = \frac{2\tau_0}{\sqrt{(A^2-1)^3}} \Theta \left(A - \frac{1+2\tau_0}{\sqrt{1+4\tau_0}} \right). \tag{7}$$

i.e. $(dP/dA)dA$ gives the probability that the magnification lies in the range $A \pm dA/2$. We will briefly discuss the effects of an inhomogeneous background mass distribution in §7.

4. Single Magnification Bias

We now consider the magnification bias (ignoring the complication of binary lenses, which as we have seen does not significantly affect the lensing rate). We compute the probability of a detectable microlensing event on the afterglow of a GRB detected at high energy. The detectability of the GRB at high energy will be affected by magnification bias as a point source. We then simply model the microlensing event as a detected GRB with a lens between 0.2 and 1.2 Einstein radii distant. The inner boundary allows a minimum time before peak magnification (so that a bump in the lightcurve can be observed), and the outer boundary simply enforces that the magnification is in excess of roughly 2 in the peak (for $w = 0.1$). The precise values of these parameters do not significantly affect our results, however, for luminosity functions with slopes $\gamma < 3$. Implicit in this prescription is the assumption that the magnification of the the gamma ray flux is the same as the magnification of the optical flux, when the optical flux is first detected. This is a good assumption as typically the afterglow would be detected in the regime where the emission region is small compared to the Einstein radius, meaning the afterglow is effectively a point source when initially detected.[5]

[5]An implicit assumption in this section is also that the optical luminosity and gamma-ray luminosity of a burst are well-correlated. In other words, in order for a burst to be detected in gamma-ray, *and* its afterglow to be observed

We now derive expressions for the number of detected sources, given lensing effects, following the discussion in Turner, Ostriker & Gott (1984). We assume a simple selection function $S(F)$ which gives the efficiency of detecting sources with flux F, and an absolute luminosity function $N(L) \equiv dn/dL$, where $F(L,z) = L/(4\pi D_L^2(z))$, and $N(L)$ is the number of sources per luminosity range. In this section and the next, we will consider bursts at a fixed redshift, thus the apparent luminosity function is trivially related to the true luminosity function. Without lensing, the number of detected sources is then

$$N_0 = \int dL S(F[L,z]) N(L). \tag{8}$$

Taking into account lensing, the number of detected sources is

$$N_{\rm lens} = \int dL S(F[L,z]) \int \frac{dA}{A} \frac{dP}{dA} N\left(\frac{L}{A}\right). \tag{9}$$

We will consider a simple power–law luminosity function, with a low– and high–flux cutoffs,

$$N(L) \propto L^{-\gamma} \Theta(L - L_{\rm L}) \Theta(L_{\rm H} - L), \tag{10}$$

and a simple choice of selection function[6]

$$S(F) = \Theta(F - F_{\rm th}), \tag{11}$$

where $F(L_{\rm H}) \equiv F_{\rm H} \gg F_{\rm th} \gg F(L_{\rm L}) \equiv F_{\rm L}$. We define $f_{\rm H} = F_{\rm th}/F_{\rm H}$ and $f_{\rm L} = F_{\rm L}/F_{\rm th}$ (we expect $f_{\rm H}, f_{\rm L} \ll 1$). Here we note that if the slope is in the range $1 < \gamma < 3$, the cutoffs can be neglected.[7] With these simple forms, we find the following expression for the unlensed source count, which of course is not measurable,

$$N_0 \propto \frac{(4\pi F_{\rm th} D_L^2)^{1-\gamma}}{\gamma - 1} \left(1 - f_{\rm H}^{\gamma-1}\right). \tag{12}$$

Not explicitly stated in Eq. 9 is the fact that one is generally interested in the number of sources with magnification larger than some value, or in some particular range. We define the quantity

$$B(A > A_0) \equiv N_{\rm lens}(A > A_0)/N_0 \tag{13}$$

---

in the optical, it is sufficient to consider the luminosity function in one waveband (in other words, a threshold in one waveband translates directly into a threshold in another waveband). We will consider in the next section the opposite case where the optical and gamma-ray flux are completely uncorrelated. Note also that, typically, observations of optical afterglows also require localization via X-ray (using BeppoSAX), making the selection process even more complicated. However, there are reasons to believe that X-ray and gamma-ray luminosities are well-correlated (Granot & Sari 2002).

[6]The realistic selection function is almost certainly more complex than a simple step function, and probably never 100% efficient even far above threshold.

[7]The $\gamma = 1$ limit comes from the convergence of the integrated luminosity function ($\int dL\, N(L)$) at the low luminosity end, while the $\gamma = 3$ limit arises from the the convergence of $\int dA\, (dP/dA)\, N(L/A)/A$ in the large A limit, where $dP/dA \propto A^{-3}$.

which is equal to the number of sources with magnification $A > A_0$, normalized by N_0, the total number of detected sources if lensing were absent (Eq. 8). With the power-law luminosity function, this takes the following form

$$B(A > A_0) = \frac{1}{1 - f_{\rm H}^{\gamma-1}} \int_{A_0}^{\infty} dA \, \frac{dP}{dA} \left[\max\left(A^{-1}, f_{\rm L}\right)^{1-\gamma} - f_{\rm H}^{\gamma-1} \right]. \tag{14}$$

We can compute $B(A > A_0)$ explicitly for the analytic $P(A)$ (Eq. 6). First, we will need the integral over the analytic probability density of an arbitrary power of amplification, given by

$$\int_{A_0}^{\infty} \frac{dA \; A^{\gamma-1}}{\sqrt{(A^2-1)^3}} = \mathcal{F}\left(\frac{3-\gamma}{2}; A_0^{-1}\right), \tag{15}$$

and we have used the definition

$$\mathcal{F}(a; x) = \frac{x^{2a}}{2a} \, {}_2\mathrm{F}_1\left(\frac{3}{2}, a; a+1; x^2\right) \tag{16}$$

with ${}_2\mathrm{F}_1$ being the standard hypergeometric function. We notice that this function has simple poles when a is a non-positive integer, and their residues are independent of x, thus when two such functions are subtracted, all poles vanish.

We define the quantity $B_0 \equiv B(A > 1)$, which gives us the ratio of the number of all detected sources taking into account lensing (with all possible magnification) to the number of all detected sources ignoring lensing. Note that by virtue of the approximation made in Eq. 7, we approximate $B(A > 1)$ by $B(A > [1 + 2\tau_0]/\sqrt{1 + 4\tau_0})$.[8] Expanding B_0 in the limit of $\tau_0 \ll 1$, we find where we have used the following expansion of $\mathcal{F}$ in the limit of small τ_0:

$$\mathcal{F}\left(a; \frac{\sqrt{1+4\tau_0}}{1+2\tau_0}\right) = \frac{1}{2\tau_0} + 1 - \frac{\sqrt{\pi}\;\Gamma(a)}{\Gamma(a-1/2)} + 2(a-1)\tau_0 + O(\tau_0^2). \tag{17}$$

We are interested in the number of microlensed sources, which we defined previously as sources falling in an annulus about a lens, with inner and outer radii of 0.2 and 1.2 in Einstein units, respectively. The number of detected microlensed sources is then just the difference of the bias factors B for minimum magnifications corresponding to the inner and outer edges of the annulus. Thus we find that the ratio of the number of microlensed sources to the number of detected sources, or equivalently the probability of a given burst being microlensed, is given by

$$P_{\rm lens} = \frac{B(A > A(1.2)) - B(A > A(0.2))}{B_0} \sim \text{several } \tau_0, \tag{18}$$

where the most naive expectation (ignoring magnification bias but taking into account lensing) is that $P_{\rm lens} = (1.2^2 - 0.2^2)\tau_0 \sim 1.4\tau_0$. In Fig. 2 we plot $P_{\rm lens}/\tau_0$ as a function of γ for several values of

[8] We have numerically checked that using the exact expression for probability $P = 1 - e^{-\tau_0 \beta^2}$ instead of $P \sim \tau_0 \beta^2$ (see Eq. 5) results in negligible changes to our results.

$f_{\rm L}$ and $f_{\rm H}$, with the constraint $f_{\rm L} f_{\rm H} = 10^{-4}$, in other words the luminosity function ranges over four orders of magnitude.[9] We have used the magnification distribution derived from the distribution in κ, though the results do not differ much from those of the analytic dP/dA. We see that the magnification bias is only significant when the slope γ becomes significantly larger than one. Note that we have fixed $\tau_0 = 1/75$ in Fig. 2, but the curves depend on the value of τ_0 only weakly. In other words, the lensing probability is nearly linear in τ_0.

Using the value of $\gamma = 1.7$ for the faint-end luminosity function from Schaefer et al. (2001), we find the magnification bias as a function of the ratios $f_{\rm L}$ and $f_{\rm H}$,

$$\frac{P_{\rm lens}}{\tau_0} = \frac{2.016 - 1.400 f_{\rm H}^{0.7}}{1 - f_{\rm H}^{0.7} + \tau_0 (1.211 - 0.538 f_{\rm L}^{1.3})}. \tag{19}$$

One can see that if $f_{\rm L}$ and $f_{\rm H}$ can be ignored, $P_{\rm lens}/\tau_0 \sim 2$. Even with this slope significantly less than three, the magnification bias causes an enhancement of the probability of a factor of roughly fifty percent. We should emphasize that magnification bias offers a smaller enhancement if γ were smaller.

5. Double Magnification Bias

In the previous section we effectively assumed that the gamma-ray / X-ray and optical luminosities were perfectly correlated. We now take the other extreme position, assuming that the gamma-ray / X-ray and optical luminosities are completely uncorrelated, though, for simplicity, both drawn from luminosity functions with the same shape but with different thresholds (see discussion in §2). It has been shown that this situation can give rise to significantly larger magnification bias (Borgeest, van Linde & Refsdal 1991; Wyithe, Winn & Rusin 2002). As before, the unlensed number counts are given by

$$N_0 = \int dL_V \, S_V(F[L_V, z]) N(L_V) \int dL_X \, S_X(F[L_X, z]) N(L_X). \tag{20}$$

where the subscripts V and X stand for the visible and X-ray wavebands relevant for selection of sources. Note that here $dL_V dL_X N(L_V) N(L_X)$ gives the number of sources with the luminosities in the two wavebands falling into the respective ranges. Taking into account lensing, the number of detected sources is

$$N_{\rm lens} = \int dL_V \, S_V(F[L_V, z]) \int dL_X \, S_X(F[L_X, z]) \int \frac{dA}{A^2} \, \frac{dP}{dA} \, N\left(\frac{L_V}{A}\right) N\left(\frac{L_X}{A}\right). \tag{21}$$

We will now define some similar variables to the previous section. We take the luminosity functions in the two bands to be identical, with the same slope and range between lower and upper cutoffs,

[9] We assume that $f_{\rm L}$ and $f_{\rm H}$, defined after Eq. 11, are both small. Their exact size, as can be seen from Fig. 2, does not matter a great deal. We choose the range $f_{\rm L} f_{\rm H}$ to span four orders of magnitude as Schaefer et al. (2001) give the luminosity function over this range. If $f_{\rm L} f_{\rm H}$ were larger, our results are not much affected.

though the detection thresholds differ.[10] We define $f_{\rm L}$ and $f_{\rm H}$ as before, based on the *smaller* detection threshold (relative to the lower luminosity function cutoff), and we define $\eta \leq 1$ as the ratio of the smaller to larger threshold. The unlensed source counts are given by

$$N_0 = \frac{(4\pi F_{\rm th} D_L^2)^{2-2\gamma}}{(\gamma-1)^2} \left(1 - f_{\rm H}^{\gamma-1}\right) \left(\eta^{\gamma-1} - f_{\rm H}^{\gamma-1}\right), \tag{22}$$

where $F_{\rm th}$ is now the lower of the two thresholds. Similarly to the previous section, we compute the excess source counts above a given magnification A_0 due to the double magnification bias, $B(A > A_0) \equiv N_{\rm lens}(A > A_0)/N_0$ (Eq. 13):

$$\begin{aligned} B(A > A_0) &= \left(1 - f_{\rm H}^{\gamma-1}\right)^{-1} \left(\eta^{\gamma-1} - f_{\rm H}^{\gamma-1}\right)^{-1} \times \\ &\int_{A_0}^{\infty} dA \, \frac{dP}{dA} \left[\max\left(A^{-1}, f_{\rm L}\right)^{1-\gamma} - f_{\rm H}^{\gamma-1}\right] \left[\max\left(\eta^{-1}A^{-1}, f_{\rm L}\right)^{1-\gamma} - f_{\rm H}^{\gamma-1}\right]. \end{aligned} \tag{23}$$

We now repeat the analysis of the previous section for the double magnification bias, with the same range of allowed magnifications, again using Eq. 19. We plot the ratio as before in Fig. 3, where we again fix $\tau_0 = 1/75$. We will take $\eta = 0.5$, and the results are insensitive to the exact value. We see that the magnification bias is insignificant for the case where $\gamma < 1$, but it can be as large as three or four in the case where $\gamma = 1.7$ (motivated by the results of Schaefer et al. 2001; see §2 for more discussions). Note that, however, if γ gets close to 2 or larger, the enhancement in lensing probability due to double magnification bias can become very large, limited only by the cut-offs in the luminosity functions – i.e. the result will be quite cut-off dependent. In fact in some cases a downturn is expected, as the very high magnification regime yields microlensing events too short to be detected. Lastly, if the two luminosity function slopes are different, the important quantity is their average, so if $(\gamma_1 + \gamma_2)/2 \to 2$, then the double magnification bias becomes large.

6. Afterglow Sample

The results of the previous two sections are valid for bursts at a single redshift only. To be more precise, we will consider a population of afterglows from a range of redshifts. We choose 27 detected afterglows as our sample, taken from Bloom et al. (2003) and listed in Table 2. While we caution that the sample is a heterogeneous one, with a probably quite complex selection process, we will continue to model only the part of the selection that has to do with the observed flux (in gamma-ray as well as in optical) – that our results are not sensitive to the precise thresholds chosen (unless γ is very close to 3 or larger for single magnification bias, or 2 or larger for double magnification

[10] Theoretically, the cutoffs for one waveband: $L_{\rm L}^V$ and $L_{\rm H}^V$, and the cutoffs for another: $L_{\rm L}^G$ and $L_{\rm H}^G$, can be completely different. What we assume here is that the range $L_{\rm H}^V/L_{\rm L}^V$ equals $L_{\rm H}^G/L_{\rm L}^G$. Our expressions here implicitly assume a rescaling has been done so that $L_{\rm L}^V = L_{\rm L}^G$ and $L_{\rm H}^V = L_{\rm H}^G$. The rescaling factors are omitted from our expressions, because they get canceled out in the end as far as the probability of lensing is concerned.

bias) will be regarded as a partial justification for our model. We calculate the microlensing optical depth as a function of redshift, as before assuming the flat $\Omega_m = 0.3$ cosmology, and assuming that the shape of the luminosity function does not evolve. For each redshift, we compute the probability of a detectable microlensed GRB. For the full sample, we then simply compute the probability that at least one observed afterglow was microlensed. In Fig. 4 we show results for various values of the thresholds, and for both $f_{\rm L} f_{\rm H} = 10^{-4}$ and $f_{\rm L} f_{\rm H} = 10^{-5}$. In principle we could use the flux information for each burst to construct a probability, but as we show in Appendix B, this would make little difference.

We have thus far assumed that lenses are uniformly distributed (i.e. not clustered), an approximation that can fail badly. For lenses distributed in isothermal galactic halos, as MACHOs would be Wyithe & Turner (2002a) found that the typical cosmological microlensing event occurs at small optical depth, and thus the isolated lens approximation is justified. In the top panel of Fig. 4 we illustrate the probability to see at least one event in the sample assuming $f = 1/15$ (MACHOs making up half of Ω_b). This probability is quite high: about 25% with no magnification bias and approaching 35% and 50% for single and double magnification bias with $\gamma = 1.7$, respectively. These probabilities make it likely that another microlensed GRBs could be observed if the sample were to be doubled.

In contrast, Wyithe & Turner (2002a) found that microlensing by stars typically occurs at optical depths of order unity, and the isolated lens approximation is not appropriate. Koopmans & Wambsganss (2001) have addressed this problem by simulating lens systems at optical depths of order unity. They find a microlensing probability proportional to optical depth for small optical depths, but turning over at optical depths around 1/10. Choosing a typical value of $\tau = 1/4$ according to Wyithe & Turner (2002a), the effectiveness of lenses is of order only one third the naive value. In discussing stellar lenses we will thus take an effective lens density $\Omega_{\rm lens,eff} \approx 10^{-3}$. In the bottom panel of Fig. 4 we illustrate the probability of observing at least one GRB lensing event due to a star in the sample. Without magnification bias, this is about 1.5%, rising to 2% and 3.5% for single and double magnification bias respectively. It thus seems unlikely that a stellar lens could be responsible.

7. Discussion and Conclusions

Our estimate of the microlensing rate for gamma ray burst afterglows is in significant disagreement with previous literature, which we outline here. If $f = 1$, then the optical depth to $z = 2$ is $\tau_0 \approx 0.2$, in significant disagreement with Koopmans and Wambsganss (2001). Computing the mean value of κ from their Eq. 4 (this is identified with our τ_0), we find $\overline{\kappa} \approx 0.04$, a factor of five smaller. They have cut their isothermal halos at radii that are too small, and have thus neglected 80% of their mass. They have done this to enforce that the halos do not overlap along the line of sight, but the fact is that they do, and significantly. They have thus underestimated the lensing probability by a factor of five. Let us explain this in more detail.

In §3 we assumed an optical depth for microlensing consistent with a uniform distribution of lenses. This is clearly not the case, as mass in clustered in halos. We assume that all of the matter is in singular isothermal sphere halos with cutoffs ($\rho(r) = \sigma^2/(2\pi G r^2)\Theta(r_0 - r)$). These will obey a luminosity–velocity dispersion relation, have luminosities taken from a Press-Schechter distribution, and have relation between cutoff radii and velocity dispersion,

$$L^\star \frac{dn}{dL} = n^\star \left(\frac{L}{L^\star}\right)^\alpha e^{-L/L^\star}, \tag{24}$$

$$\frac{L}{L^\star} = \left(\frac{\sigma}{\sigma^\star}\right)^\gamma, \tag{25}$$

$$\frac{r_0}{r_0^\star} = \left(\frac{\sigma}{\sigma^\star}\right)^\beta. \tag{26}$$

Following Koopmans & Wambsganss (2001), we will take $\alpha = -1$, $\gamma = 4$, as the fiducial case, with $n^\star = 0.0061\,h^3$ Mpc^{-3}, $\sigma^\star = 225$ km s^{-1}. To prescribe the cutoff radii, we take $\beta = 1$, but the results are insensitive to the precise value of beta as long as it is not close to zero. We will compute $r_0^\star$ by normalizing the total mass density to account for $\Omega_m = 0.3$, namely all mass lies in halos. We find

$$r_0^\star = \left(\frac{3}{16\pi}\right) \frac{\Omega_m H_0^2}{n^\star \sigma^{\star 2}} \Gamma\left(1 + \alpha + \frac{2+\beta}{\gamma}\right)^{-1} = 0.47\ h^{-1}\ \mathrm{Mpc}. \tag{27}$$

We now can easily compute the geometric cross section of halos, and the mean number of halos intersected on a line of sight to a particular redshift,

$$\tau_{\rm GEOM} = \left(\frac{2\pi}{3}\right)\left(\frac{n^\star r_0^{\star 2} c}{\Omega_m H_0}\right) \Gamma\left(1 + \alpha + 2\beta/\gamma\right) \left(\sqrt{\Omega_m (1+z)^3 + \Omega_\Lambda} - 1\right), \tag{28}$$

$$= 50.7 \left(\sqrt{\Omega_m (1+z)^3 + \Omega_\Lambda} - 1\right). \tag{29}$$

Even to moderate redshift, a significant number of halos are intersected. For GRB 000301C at $z = 2.034$, $\tau_{\rm GEOM} \approx 100$, and the approximation that halos do not overlap is therefore not accurate. This is the origin of our disagreement.

We have shown that a large number of halos are typically intersected. However, there will be variations in the optical depth (or equivalently, convergence) between lines of sight. We have done a simple test, simulating the distribution of convergences and modifying the magnification distribution dP/dA accordingly. The magnification bias we find does not vary by more than 15% in this case.

We have shown that the consideration of magnification bias (both single and double) is important, in that the expected probability that a given observed gamma ray burst is microlensed can be roughly three times the naive optical depth estimate. MACHOs making up half of the baryonic matter have a significant probability to cause such an event, but we find that stellar lenses alone have a very small probability (less than 3% for any event in the afterglow sample) to do so. We find that binaries can affect the gamma ray burst microlensing rate at the 25% level, which though surprisingly large, is not very significant.

A single observed event with a low probability is not in itself problematic. However, should another microlensed gamma ray burst be observed in another thirty afterglows, we believe it would be a significant indication that there are significantly more lenses in the universe than can be inferred from stars. In that case, the effects we have calculated could be quite important in determining the exact density of lenses.

We thank Jules Halpern for numerous enlightening discussions, and Andrei Gruzinov, Leon Koopmans, Pawan Kumar, Dani Maoz, Re'em Sari and Eli Waxman for useful conversations. EAB acknowledges support from the Columbia University Academic Quality Fund. LH acknowledges support by an Outstanding Junior Investigator Award from the DOE, grant AST-0098437 from the NSF and grant NAG5-10842 from NASA. This research was supported in part by the NSF under grant PHY99-07949 at the Kavli Institute for Theoretical Physics at the University of California, Santa Barbara.

A. Binary Lenses

We discuss the two point mass gravitational lens, a model that has been studied extensively (Schneider & Weiß 1986; Erdl & Schneider 1993). We quote some relevant results. We take the masses of the lenses to be M_1 and M_2, with $M = M_1 + M_2$, and we define dimensionless masses $\nu_{1,2} = M_{1,2}/M$ such that $\nu_1 + \nu_2 = 1$. Furthermore, we define $q = M_2/M_1$, with $0 \leq q \leq 1$ without loss of generality. Note that taking $q = 0$ yields the single point mass lens.

The excess optical depth due to binaries is given by

$$\frac{\Delta\tau}{\tau} = \frac{\tau_{2*} - \tau_{1*}}{\tau_{1*}} = \frac{\beta_{2*}^2}{\beta_{1*}^2} - 1. \tag{A1}$$

For the binary systems, we take a distribution flat in $q \equiv M_2/M_1$, and also flat in $\log d$, where d is the projected separation of the lenses on the sky, for the ensemble average (Baltz & Gondolo 2001).

We adopt a complex parameterization (Witt 1990) of the lens system. We introduce complex angular coordinates on the plane of the sky, $z = (\theta_x + i\theta_y)/\theta_E$. Given two lenses at angular positions z_1 and z_2, a source at ζ will have images at the solutions z of the lens equation

$$\zeta = z - \overline{\alpha(z)} = z - \frac{\nu_1}{\overline{z} - \overline{z}_1} - \frac{\nu_2}{\overline{z} - \overline{z}_2}. \tag{A2}$$

In this formalism, the Jacobian of $\zeta(z)$ in Eq. A2 is

$$J(z) = 1 - \left|\frac{\partial\alpha}{\partial z}\right|^2. \tag{A3}$$

The magnification of an image at z of a point source at ζ is given by $1/|J(z)|$, with the sign of $J(z)$ giving the parity p of the image. The total magnification is the sum of the individual magnifications of the images.

For a source of uniform surface brightness, the magnification is just the image area divided by the source area (Gould & Gaucherel 1997),

$$\mu = \int_0^{2\pi} d\phi \, \mathrm{Im}\left[\sum_i p_i \overline{z}_i \frac{dz_i}{d\phi}\right] \Bigg/ \int_0^{2\pi} d\phi \, \mathrm{Im}\left[\overline{\zeta}\frac{d\zeta}{d\phi}\right]. \tag{A4}$$

We never need to use numerical differencing as long as we can analytically differentiate the expression for the source boundary $\zeta(\phi)$. As we are concerned with annular sources, the source boundaries will always have the form $\zeta = \zeta_0 + re^{i\phi}$, which can be easily differentiated. Differentiating the lens equation, we find

$$\frac{d\zeta}{d\phi} = \frac{dz}{d\phi} - \overline{\frac{\partial\alpha}{\partial z}\frac{dz}{d\phi}}, \tag{A5}$$

Solving for $dz/d\phi$, we find the following result, depending only on the numerical solution of the lens equation, and not on any numerical derivatives

$$\frac{dz}{d\phi} = \frac{1}{J(z)}\left(\frac{d\zeta}{d\phi} + \overline{\frac{\partial\alpha}{\partial z}\frac{d\zeta}{d\phi}}\right). \tag{A6}$$

We can take care of the required parities trivially. Since we effectively need $p_i \, dz_i/d\phi$, we simply take the absolute value of the Jacobian factor $J(z)$ in Eq. A6, since $p_i = \mathrm{sign}\, J(z_i)$.

B. Flux Information

Given that we have the gamma ray fluxes for this sample of bursts, we could consider using that information in the determination of the probability. In particular, we could write the probability for an observed burst with apparent flux F_i and redshift z_i,

$$P_{\rm lens}(F_i, z_i) = \frac{\int_{A_{1.2}}^{A_{0.2}} dA \, (dP/dA) \, N(L(F_i, z_i)/A)/A}{\int_1^\infty dA \, (dP/dA) \, N(L(F_i, z_i)/A)/A}. \tag{B1}$$

This compares with Eq. 18 for the single magnification bias, which can be written in a similar form

$$P_{\rm lens}(z_i) = \frac{\int_{A_{1.2}}^{A_{0.2}} dA \, (dP/dA)/A \int_{F_{\rm th}}^\infty dF \, N(L(F, z_i)/A)}{\int_1^\infty dA \, (dP/dA)/A \int_{F_{\rm th}}^\infty dF \, N(L(F, z_i)/A)}. \tag{B2}$$

For a power law luminosity function with no cutoffs, as is approximately the case when $1 < \gamma < 3$, these two probabilities are identical burst by burst. Summing over the sample reduces the small discrepancy between them when the luminosity function is not a pure power law.

REFERENCES

Baltz, E. A. & Gondolo, P. 2001, ApJ, 559, 41

Bloom, J. S., Frail, D. A. & Kulkarni, S. R. 2003, ApJ, 594, 674

Borgeest, U., van Linde, J. & Refsdal, S. 1991, A&A, 251, L35

Dalcanton, J. J., Canizares, C. R., Granados, A., Steidel, C. C. & Stocke, J. T. 1994, ApJ, 424, 550

Erdl, H. & Schneider, P. 1993, A&A, 268, 453

Fields, B. D., Freese, K. & Graff, D. S. 2000, ApJ, 534, 265

Frail, D. A. et al. 2001, ApJ, 562, L55

Freedman, D. L. & Waxman, E. 2001, ApJ, 547, 922

Fukugita, M., Hogan, C. J. & Peebles, P. J. E. 1998, ApJ, 503, 518

Garnavich, P. M., Loeb, A. & Stanek, K. Z. 2000, ApJ, 544, L11

Graff, D. S., Freese, K., Walker, T. P. & Pinsonneault, M. H. 1999, ApJ, 523, L77

Granot, J. & Loeb, A. 2001, ApJ, 551, L63

Granot, J., Piran, T. & Sari, R. 1999, ApJ, 527, 236

Granot, J. & Sari, R. 2002, ApJ, 568, 820

Gaudi, B. S., Granot, J. & Loeb, A. 2001, ApJ, 561, 178

Gaudi, B. S. & Loeb, A. 2001, ApJ, 558, 643

Ioka, K. & Nakamura, T. 2001, ApJ, 561, 703

Koopmans, L. V. E. & Wambsganss, J. 2001, MNRAS, 325, 1317

Krumholz, M., Thorsett, S. E. & Harrison, F. A. 1998, ApJ, 506, L81

Kulkarni, S. R., et al. 1998, Nature, 393, 35

Kumar, P. 2000, ApJ, 538, L125

Loeb, A. & Perna, R. 1998, ApJ, 495, 597

Madau, P., Ferguson, H. C., Dickinson, M. E., Giavalisco, M., Steidel, C. C. & Fruchter, A. 1996, MNRAS, 283, 1388

Madau, P., Pozzetti, L., & Dickinson, M. 1998, ApJ, 498, 106

Mao, S. & Loeb, A. 2001, ApJ, 547, L97

Metzger, M. R., Djorgovski, S. G., Kulkarni, S. R., Steidel, C. C., Adelberger, K. L., Frail, D. A., Costa, E. & Fronterra, F. 1997, Nature, 387, 879

Panaitescu, A. 2001, ApJ, 556, 1002

Press, W. H. & Gunn, J. E. 1973, ApJ, 185, 397

Rutledge, R. E., Hui, L., & Lewin, W. H. G. 1995, MNRAS, 276, 753

Sari, R., Piran, T., & Narayan, R. 1998, ApJ, 497, L17

Schaefer, B. E., Deng, M. & Band, D. L. 2001, ApJ, 563, L123

Schneider, P. & Weiß, A. 1986, A&A, 164, 237

Turner, E. L., Ostriker, J. P. & Gott, J. R. 1984, ApJ, 284, 1

Waxman, E. 1997a, ApJ, 489, L33

Waxman, E. 1997b, ApJ, 491, L19

Wijers, R. A. M. J., Bloom, J. S., Bagla, J. S. & Natarajan, P. 1998, MNRAS, 294, L13

Witt, H. J. 1990, A&A, 236, 311

Wyithe, J. S. B. & Turner, E. L. 2002a, ApJ, 567, 18

Wyithe, J. S. B. & Turner, E. L. 2002b, ApJ, 575, 650

Wyithe, J. S. B., Winn, J. N. & Rusin, D. 2003, ApJ, 583, 58

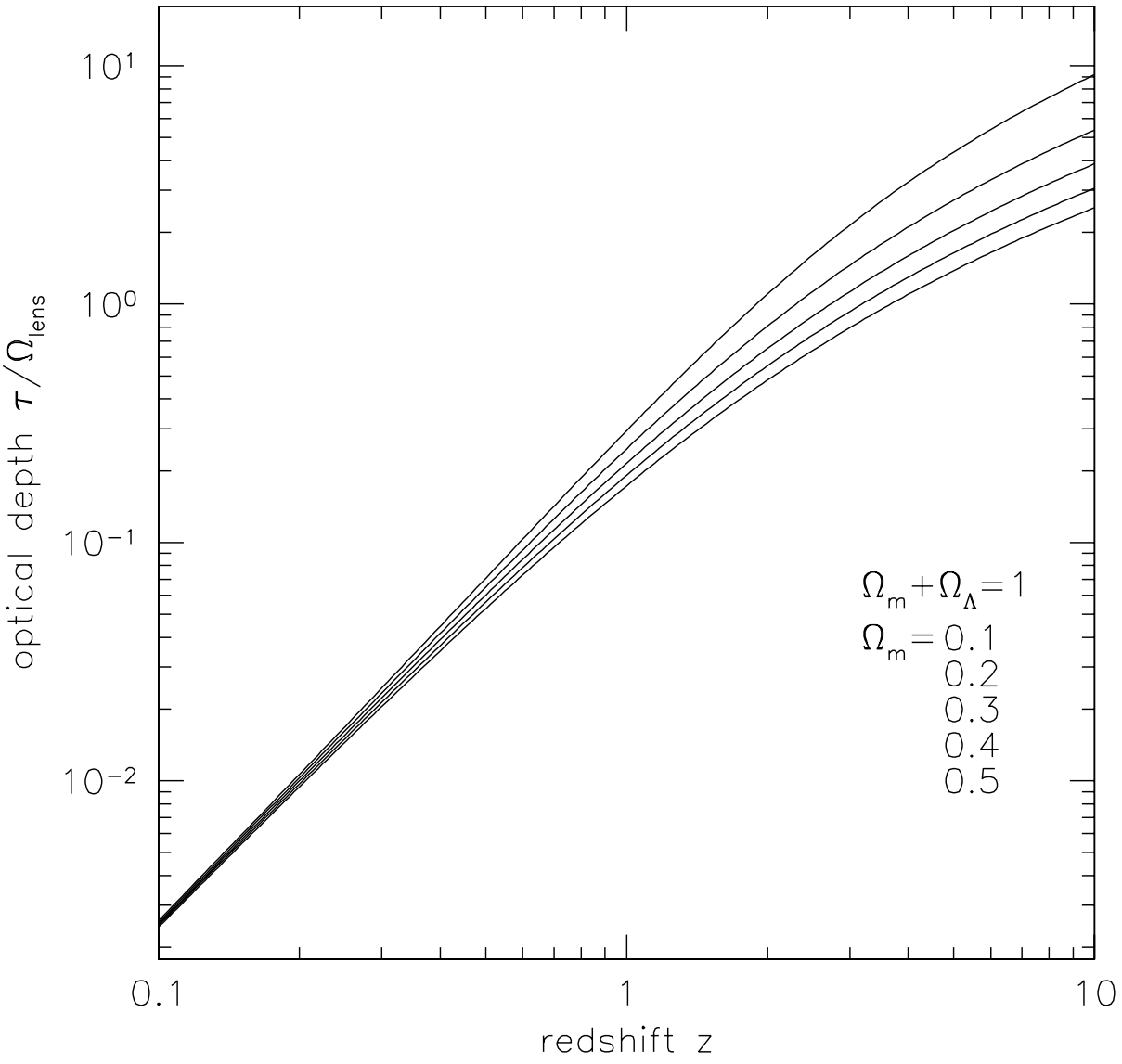

Fig. 1.— Optical depth for microlensing for several values of Ω_m in a flat cosmology. We have divided out the $\Omega_{\rm lens}$ dependence. The curves from top to bottom correspond to $\Omega_m = 0.1$ to 0.5 in steps of 0.1. For our fiducial case of $\Omega_m = 0.3$ and $z = 2$, we find $\tau = 0.65\,\Omega_{\rm lens}$.

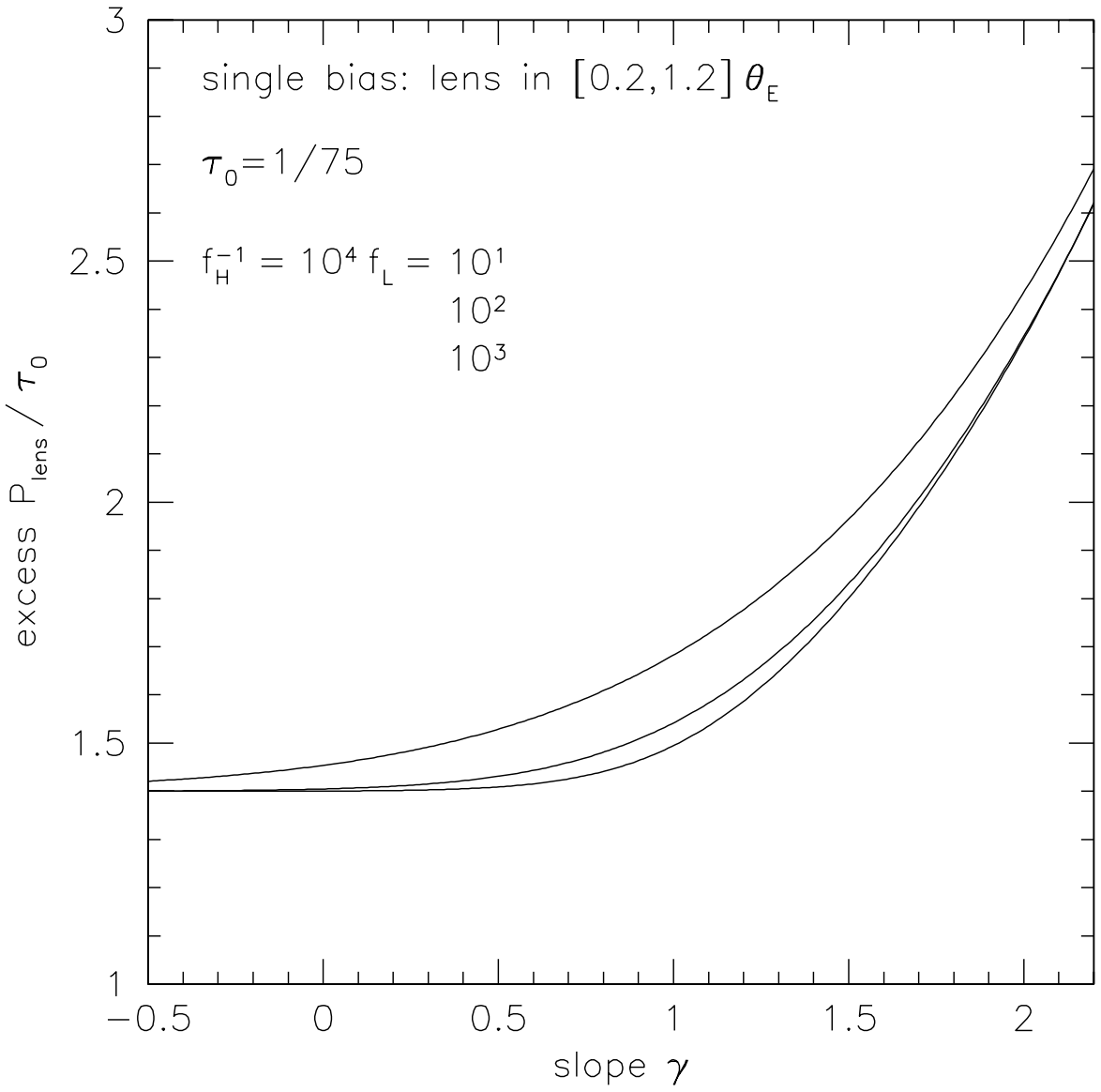

Fig. 2.— Magnification bias as a function of the luminosity function slope. We have illustrated three possibilities for the high– and low–luminosity cutoff. The value of this cutoff is not very significant when γ is not near three. The curves are, top to bottom, $f_{\rm H} = 0.1, 0.01, 0.001$, and we thus see that the effect of magnification bias is largest when the threshold is not too far from the maximum luminosity ($f_{\rm H}$ not too much smaller than unity).

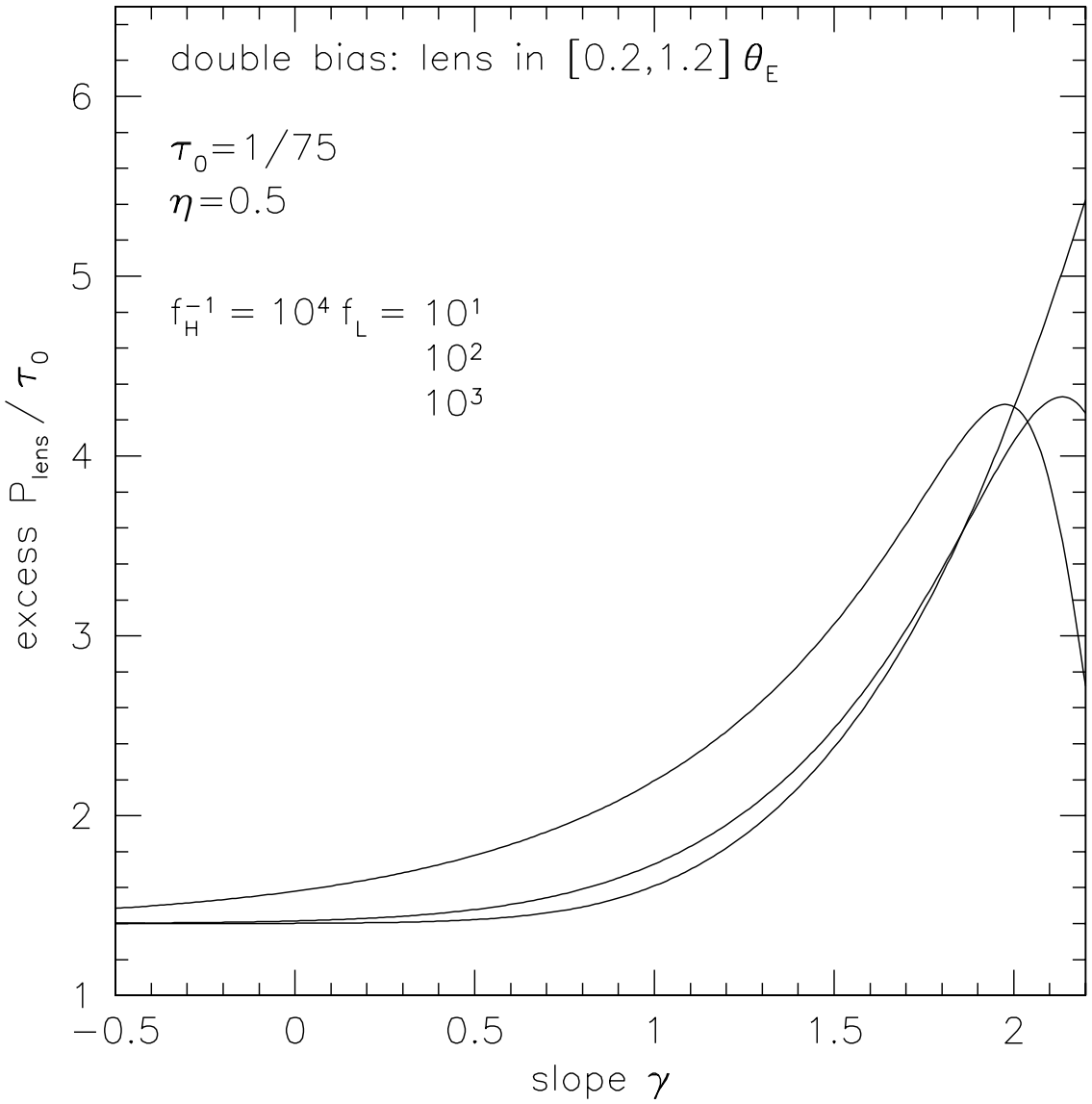

Fig. 3.— Double magnification bias as a function of the luminosity function slope. We have used the same three possibilities for the high– and low–luminosity cutoff as in Fig. 2. The value of this cutoff is not very significant unless γ is larger than two. The curves match those in Fig. 2.

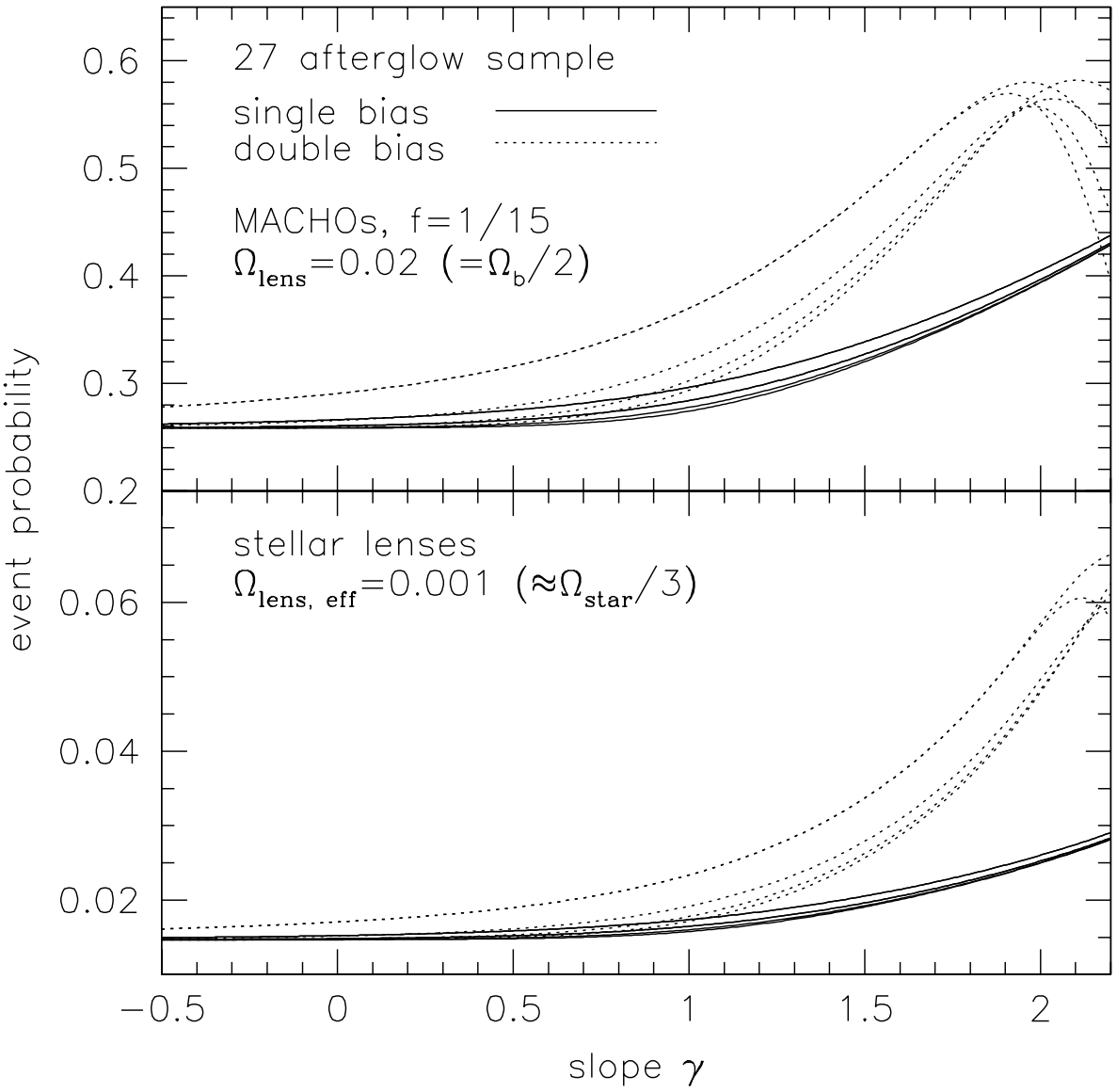

Fig. 4.— Probability of at least one microlensing event in the sample. 27 afterglows with well–determined redshifts are considered, adjusting the optical depth and thresholds according to cosmology only. Several curves are shown for both the single and double magnification bias cases. In the top panel, we illustrate MACHO lensing where $\Omega_{\rm lens} = 0.02$, namely half of the baryons in the universe. In the bottom panel, we illustrate stellar lensing, accounting for the fact that stars are less effective per mass as they are strongly clustered (Wyithe & Turner 2002a; Koopmans & Wambsganss 2001). This is a somewhat crude estimate, and accordingly we have used the analytic dP/dA. As in Figs. 2-3, the higher probability curves correspond to the largest $f_{\rm H}$ (though still small compared with unity). Changing the range of luminosity function ($f_{\rm L} f_{\rm H} = 10^{-4}, 10^{-5}$) has only a small effect in that the excess probability function turns over at slightly smaller slopes for the $f_{\rm L} f_{\rm H} = 10^{-5}$ case.

Table 1. Optical Depth for Binary Lensing of GRBs

threshold magnification	$w = 0.20$			$w = 0.10$			$w = 0.05$		
	β_{1*}^2	β_{2*}^2	$\Delta\tau/\tau$	β_{1*}^2	β_{2*}^2	$\Delta\tau/\tau$	β_{1*}^2	β_{2*}^2	$\Delta\tau/\tau$
5.0	0.135	0.142	4.93%	0.145	0.179	23.6%	0.185	0.259	40.0%
3.0	0.341	0.359	5.22%	0.459	0.525	14.4%	0.599	0.763	27.3%
2.0	1.007	1.134	1.77%	1.399	1.503	7.47%	1.849	2.121	14.7%
1.5	2.785	2.793	0.30%[a]	4.022	4.111	2.21%	5.534	5.901	6.63%

[a]The Monte Carlo errors in the computed values of $\Delta\tau/\tau$ are as large as a few tenths of a percent, thus this result is marginally consistent with no enhancement due to binary lenses.

Note. — Optical depth is given by $\tau = \tau_0\beta_{n*}^2$. The values of β_{2*} are calculated assuming that binary systems with separations differing from unity by more than half of an order of magnitude act as single lenses. We thus slightly underestimate the effect of binary lenses.

Table 2. Sample of GRB Afterglows

GRB	redshift	χ	$(H_0 D_L/c)^2$	Approximate Fluence (10^{-6} erg cm^{-2})	Scaled Fluence (10^{-6} erg cm^{-2})
970228	0.695	0.5817	0.972	11.0	10.69
970508	0.835	0.6730	1.525	3.17	4.834
970828	0.958	0.7473	2.141	96.0	205.5
971214	3.418	1.5712	48.19	9.44	454.9
980613	1.096	0.8245	2.987	1.71	5.108
980703	0.966	0.7519	2.185	22.6	49.38
990123	1.600	1.0609	7.608	268.	2040.
990506	1.300	0.9280	4.556	194.	883.9
990510	1.619	1.0687	7.834	22.6	177.0
990705	0.840	0.6762	1.548	93.0	144.0
990712	0.433	0.3888	0.310	6.50	2.015
991208	0.706	0.5891	1.010	100.	101.0
991216	1.020	0.7827	2.500	194.	485.0
000131	4.500	1.7496	92.60	41.8	3871.
000210	0.846	0.6801	1.577	61.0	96.20
000301C	2.034	1.2208	13.72	4.10	56.25
000418	1.119	0.8367	3.143	20.0	62.86
000911	1.059	0.8041	2.740	230.	630.2
000926	2.037	1.2218	13.77	6.20	85.37
010222	1.477	1.0089	6.244	120.	749.3
010921	0.451	0.4029	0.342	15.4	5.267
011121	0.362	0.3312	0.203	24.0	4.872
011211	2.140	1.2552	15.53	5.00	77.65
020405	0.690	0.5782	0.955	38.0	36.29
020813	1.254	0.9057	4.167	38.0	158.3
021004	2.332	1.3135	19.15	3.20	61.28
021211	1.006	0.7748	2.416	1.00	2.416

Note. — Redshifts, coordinate distance, luminosity distance, and observed and scaled fluence are given. The redshifts and fluences are taken from Bloom et al. (2003).